

## Research Article

# Focused Fluid Flow, Shallow Gas Hydrate, and Cold Seep in the Qiongdongnan Basin, Northwestern South China Sea

Minghui Geng <sup>1,2</sup>, Ruwei Zhang <sup>1,2</sup>, Shengxiong Yang <sup>1,2</sup>, Jun Guo <sup>1,2</sup>,  
and Zongheng Chen <sup>1,2</sup>

<sup>1</sup>MNR Key Laboratory of Marine Mineral Resources, Guangzhou Marine Geological Survey, China Geological Survey, Guangzhou 510760, China

<sup>2</sup>Southern Marine Science and Engineering Guangdong Laboratory, Guangzhou 511458, China

Correspondence should be addressed to Ruwei Zhang; [cgszrw@163.com](mailto:cgszrw@163.com)

Received 24 January 2021; Revised 7 May 2021; Accepted 24 May 2021; Published 12 June 2021

Academic Editor: Zhifeng Wan

Copyright © 2021 Minghui Geng et al. This is an open access article distributed under the Creative Commons Attribution License, which permits unrestricted use, distribution, and reproduction in any medium, provided the original work is properly cited.

The 3D seismic data acquired in the central Qiongdongnan Basin, northwestern South China Sea, reveal the presence of shallow gas hydrate, free gas, and focused fluid flow in the study area, which are indicated by multiple seismic anomalies, including bottom simulating reflectors, polarity reverses, pull-downs, minor faults, and gas chimneys intensively emplaced within the shallow strata. A new cold seep is also discovered at approximately 1520 m water depths with an ~40 m wide crater in the west part of the study area. Water column imaging, seafloor observation, and sampling using the remotely operated vehicle “Haima” demonstrate ongoing gas seepages and shallow gas hydrates at this site. Thermogenic gas in the study area migrates from the deep reservoir through the gas hydrate stability zone along deep faults and gas chimneys, forms shallow gas hydrate and free gas, and sustains localized gas seepage within this cold seep. The results provide insight into the relationship between shallow gas hydrate accumulation and deep hydrocarbon generation and migration and simultaneously have important implications for hydrocarbon explorations in the Qiongdongnan Basin, northwestern South China Sea.

## 1. Introduction

According to hydrocarbon supplies and metallogenic characteristics, gas hydrates can be characterized into two categories: diffusive and leakage types. The diffusive gas hydrates markedly indicated by bottom simulating reflectors (BSRs) dominantly develop in the Shenhu area, northern South China Sea (SCS), and have received extensive and comprehensive research studies [1–3]. Moreover, both the Shenhu area and the deepwater slope area of the Qiongdongnan Basin (QDNB) provide favorable conditions for leakage gas hydrate formation. The leakage gas hydrates are commonly related to focused fluid flows [4–6] or/and cold seeps [7, 8] at many active and passive continental margins around the world. The leakage gas hydrate deposit zone is between the seafloor and the base of the gas hydrate stability zone (BGHSZ) [9–11], commonly has high methane flux and coexists with free gas [12]. Gas hydrate destabilization may

occur and release methane which migrates along faults, fractures, pipes, mud diapirs, gas chimneys, etc., into oceans and will nourish cold seeps on the seafloor.

The shallow gas hydrates in the QDNB belong to the leakage type, and their accumulation within the shallow marine sediments is attributed to focused fluid flows in the basin [8, 13]. Active cold seeps in the SCS have been reported as northwestern “Haima” cold seeps [14] and northeastern site F [15, 16]. Now, a new and active cold seep is found, approximately 50 km northeast of the “Haima” cold seeps. In this paper, we aim to study the distributions and subsurface features of the shallow gas hydrates, focused fluid flows, and cold seep in the QDNB, northwestern SCS, by use of 3D seismic data acquired in 2018. Based on the new results, the relationship between shallow gas hydrate accumulation and deep hydrocarbon generation and migration is discussed. Furthermore, the newly discovered cold seep is also briefly presented.

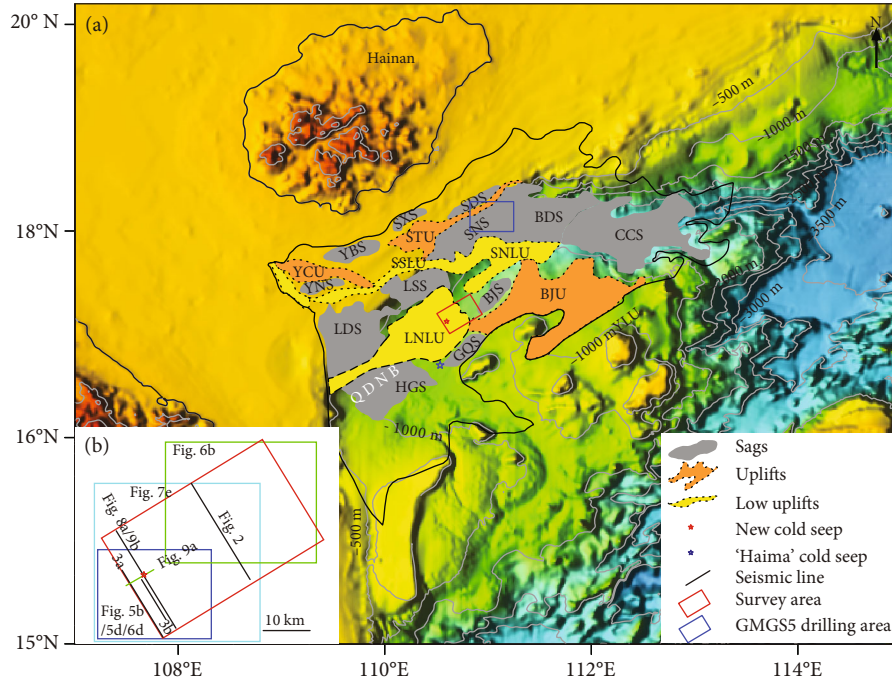


FIGURE 1: (a) The study area in the QDNB and (b) its corresponding amplified map. The black lines in panel (a) mark the boundary of the QDNB. The gray, orange, and yellow areas indicate sags, uplifts, and low uplifts in the basin, respectively. The red and blue rectangles show the study area and the GMGS5 drilling area, respectively. The red and blue stars label the newly discovered and “Haima” cold seeps, respectively. The black and green lines in panel (b) mark the seismic lines and echogram, respectively. The blue, cyan, and green areas indicate the locations of Figures 5(b), 5(d), and 6(d), Figure 7(e), and Figure 6(b), respectively. BJS: Beijiao Sag; BDS: Baodao Sag; CCS: Changchang Sag; GQS: Ganquan Sag; HGS: Huaguang Sag; LDS: Ledong Sag; LSS: Lingshui Sag; SDS: Songdong Sag; SNS: Songnan Sag; SXS: Songxi Sag; YBS: Yabei Sag; YNS: Yanan Sag; BJU: Beijiao Uplift; STU: Songtao Uplift; YCU: Yacheng Uplift; YLU: Yongle Uplift; LNLU: Lingnan Low Uplift; LSLU: Lingshui Low Uplift; SNLU: Songnan Low Uplift.

## 2. Geological Settings

The QDNB is a Cenozoic basin located in the intersection of the northern SCS passive continental margin and the strike-slip Red River fault zone. The basin has experienced two main geological evolutionary stages [17–21]: (1) rift stage (Eocene-Oligocene): during this period, a series of half-grabens, grabens, and composite structures form in the basin; and (2) postrift thermal subsidence (Miocene-Quaternary): since Late Miocene, accelerated postrift subsidence occurs in the basin [22, 23] and generates 5000–9000 m thick marine sediments, which are dominated by neritic and bathyal mudstones, the important and main source rocks of the basin [24, 25]. In addition, the basin is characterized by overpressure [26–29], high sedimentation rates [22, 30], and high thermal gradients [24, 31], which jointly promote hydrocarbon generation.

The QDNB structural framework is constituted by three depressions and two uplifts: the northern depression, the northern (central) uplift, the central depression, the southern uplift, and the southern depression, which can be further divided into different sags and uplifts of third-order structural regions [29, 32]. The study area covers an area of 800 km<sup>2</sup> and lies in the central depression, with a relatively flat topography at water depths ranging from 1450 m to 1700 m (Figure 1). Most of the study area lies in the Lingnan Low Uplift, and the rest includes part of the transitional zones

between the Lingnan Low Uplift and the Beijiao Sag. Since Late Miocene, the whole study area is in the subsidence stage with a thick sequence of marine sediments and generates large amounts of thermogenic hydrocarbons. Seafloor spreading in the SCS results in extensive normal faults (Figure 2) [33], which can provide pathways for the upward migration of deep gas and fluids. Tectonic activities in the QDNB have become weak since Pliocene [33], and hence, almost all normal faults do not extend to the seafloor [28].

We have no access to the borehole data in the study area and cannot directly estimate the seismic sequence ages. Hence, we collect and analyze previous seismic interpretations [22, 25] and well data from adjacent regions [8, 34]. According to the unconformities and the seismic reflection characteristics of conformable interfaces, we have identified seven reflecting horizons ( $T_0$ – $T_g$ ), which divide the basin strata into 6 sequences (Figure 2), including the E-O (Eocene-Oligocene,  $T_g$ – $T_{60}$ ), LM (Lower Miocene,  $T_{60}$ – $T_{50}$ ), M (Middle Miocene,  $T_{40}$ – $T_{50}$ ), UM (Upper Miocene,  $T_{30}$ – $T_{40}$ ), P (Pliocene,  $T_{20}$ – $T_{30}$ ), and Q (Quaternary,  $T_0$ – $T_{20}$ ) Series.

## 3. Data and Method

Here, we mainly utilize the 3D seismic data to analyze the distributions, the characteristics, and the subsurface structures

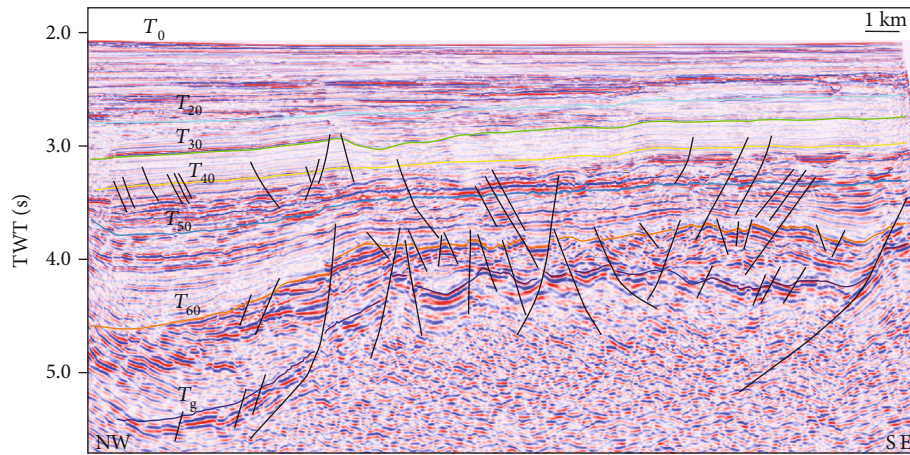
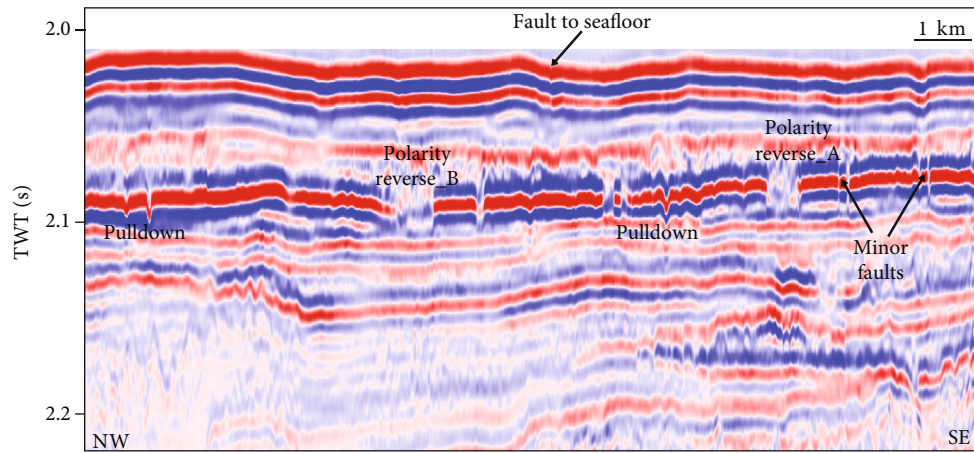
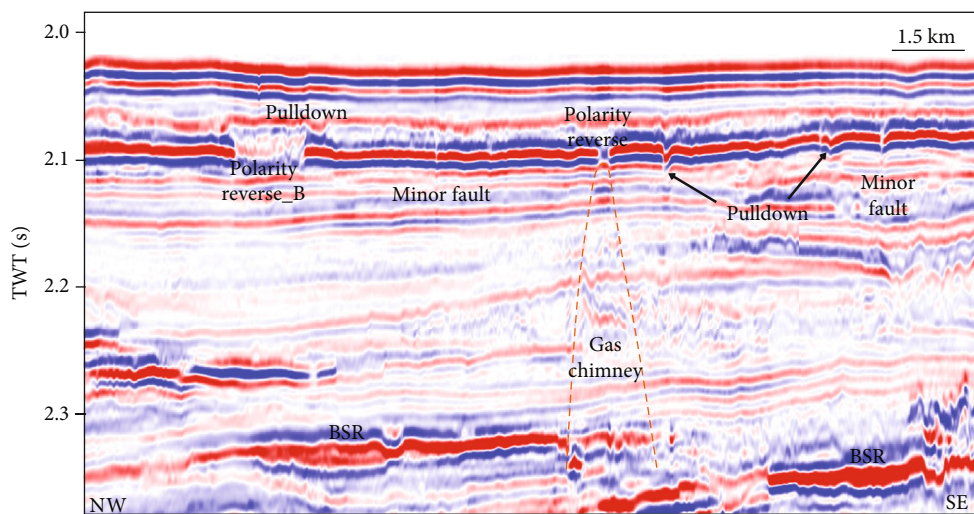


FIGURE 2: Sedimentary filling in the study area. The black lines indicate faults. The colorful solid lines represent seven seismic reflecting interfaces. Six sequences E-O (Eocene-Oligocene,  $T_g$ - $T_{60}$ ), LM (Lower Miocene,  $T_{60}$ - $T_{50}$ ), M (Middle Miocene,  $T_{40}$ - $T_{50}$ ), UM (Upper Miocene,  $T_{30}$ - $T_{40}$ ), P (Pliocene,  $T_{20}$ - $T_{30}$ ), and Q (Quaternary,  $T_0$ - $T_{20}$ ) Series are marked in the section.



(a)



(b)

FIGURE 3: Seismic anomalies shown in the sections (see their locations in Figure 1(b)).

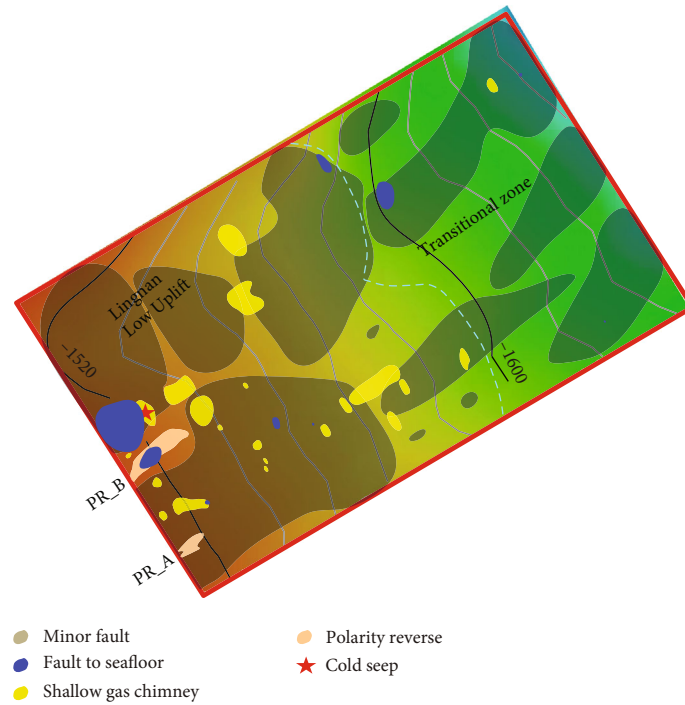


FIGURE 4: Distribution of the seismic anomalies in the study area.

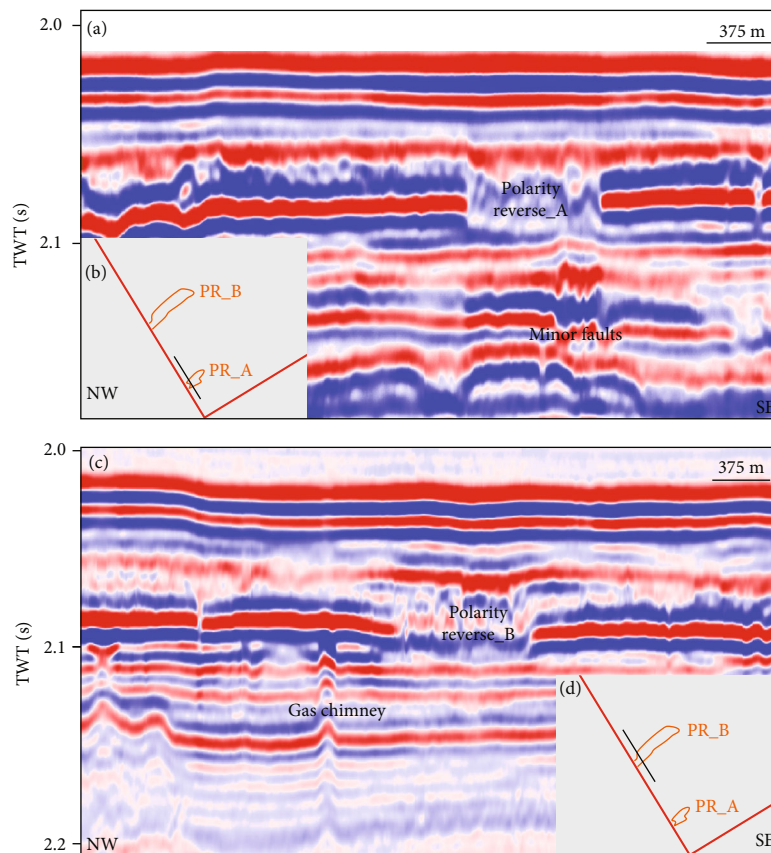


FIGURE 5: (a, c) Seismic sections and (b, d) distributions of the polarity reverse\_A (PR\_A) and polarity reverse\_B (PR\_B) in the study area. The black lines in panels (b) and (d) represent the seismic lines, the red lines represent the study area boundaries, and the polarity reverse zones indicated by the orange areas are located in the southwestern study area.

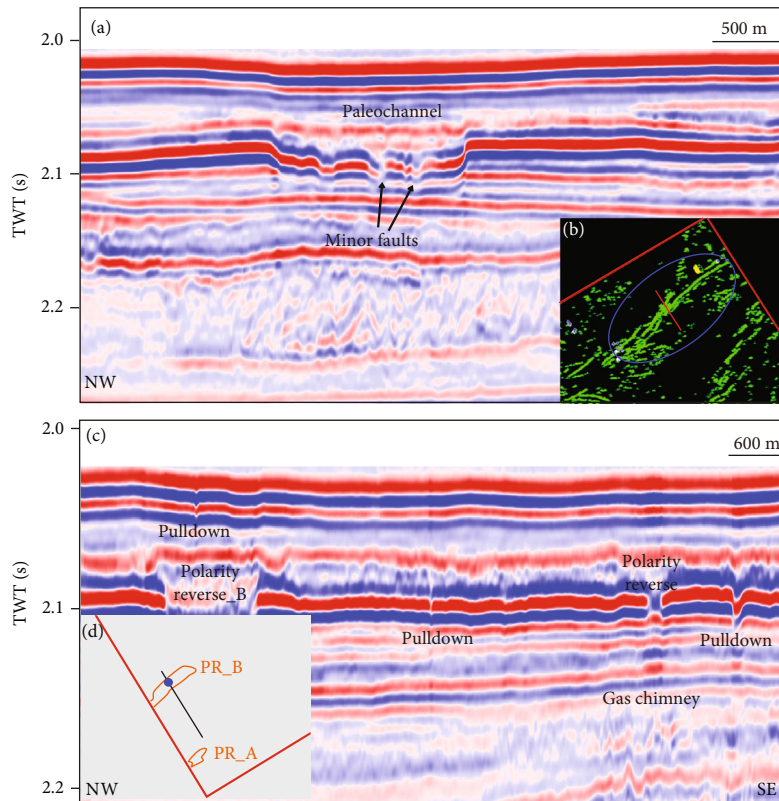


FIGURE 6: (a, c) Seismic sections and (b, d) distributions of the minor faults and pulldowns in the study area. The red line in panel (b) represents the seismic section shown in panel (a). The green points and blue oval indicate the minor faults and paleochannel, respectively. The black line in panel (d) represents the seismic section shown in panel (c), and the orange areas indicate the polarity reverse zones in the study area. The blue point indicates the location of the pulldown above the PR\_B.

of the shallow gas hydrates, the focused fluid flows, and the newly discovered cold seep in the central QDNB. The 3D seismic data were acquired in 2018 by the Bureau of Geophysical Prospecting Inc. “Pioneer” vessel. In total, an area of 800 km<sup>2</sup> was surveyed using 6 parallel streamers with intervals of 112.5 m. The streamers are 5100 m long with 816 channels (group interval 6.25 m). Three GI guns with a volume of 1960 cubic inches and an interval of 37.5 m are alternatively triggered at a shot point distance of 37.5 m. The 3D seismic data has inline (NW-SE) and crossline (SW-NE) spacings of 18.75 and 3.125 m, respectively, and a 1.0 ms sampling interval. They go through a precise data processing procedure, and the seismic interval velocities of 1400–2000 m/s for the shallow strata and the 40 Hz dominant frequency yield a vertical resolution of 8.75–12.5 m [35], which explicitly image the subsurface structures of the shallow gas hydrates and focused fluid flows in the study area. In addition, the water column imaging, seafloor observations, and samplings using the remotely operated vehicle (ROV) “Haima” are used to describe the newly discovered cold seep. A multibeam echo sounder provides an efficient method for hydroacoustic detection, which is a first-order remote proof of active gas seepage at the cold seep. The impedance contrasts between the water and gas bubbles released from cold seeps bring about strong backscattering of the transmitted acoustic wave, which will create gas flares in echograms [7].

## 4. Results

**4.1. Focused Fluid Flows, Shallow Gas Hydrates, and Free Gas in the Study Area.** A variety of seismic anomalies are observed in the 3D seismic sections (Figures 3 and 4), including polarity reverses, pulldowns, minor faults, gas chimneys, and BSRs, which indicate the presence of focused fluid flows, free gas, and shallow gas hydrates in the central QDNB, northwestern SCS.

The first type of seismic anomaly is polarity reverse. It marks a localized decrease in acoustic impedance (the product of velocity times density) [36, 37], which indicates the presence of free gas in the strata [38]. The sediment interface in the shallow strata is normally displayed in the seismic section as a positive polarity reflection; however, polarity reverses break the continuous reflection event and exhibit a negative seismic phase (Figures 3 and 4). Large-scale polarity reverse zones in the study area mainly include the polarity reverse\_A (PR\_A) and the polarity reverse\_B (PR\_B) and else may occur at the top of gas chimneys (Figure 3(b)). The PR\_A and PR\_B are all located in the southwestern part of the study area, with an area of 1.516 km<sup>2</sup> and 5.648 km<sup>2</sup>, respectively (Figures 4, 5(b), and 5(d)). Both of them are emplaced at similar depths, within the Quaternary strata, between 2060 ms and 2110 ms TWT (Two-Way Travel Time) below the seafloor, and are connected to the

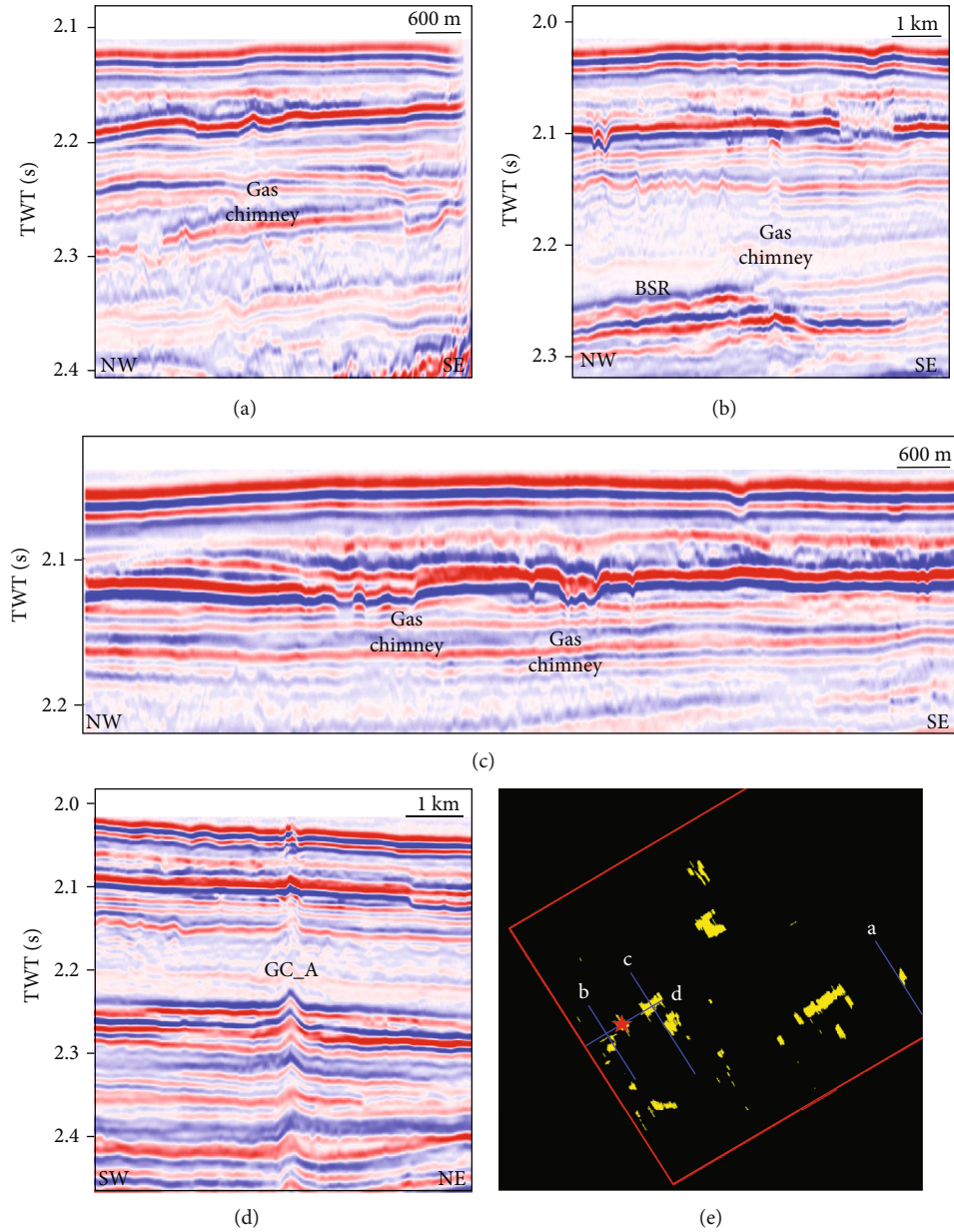


FIGURE 7: (a–d) Seismic sections and (e) distributions of the shallow gas chimneys in the study area. The yellow areas in panel (e) indicate shallow gas chimneys, the blue lines represent seismic lines shown in panels (a–d), and the red star labels the newly discovered cold seep.

underlying strata through minor faults or shallow gas chimneys (Figures 5(a) and 5(c)), which may serve as pathways for gas migration.

Minor faults are the most widely distributed features in the study area and cover more than half of the study area (Figure 4). They are proved to play important roles in gas accumulations and gas hydrate deposits, as they provide focused fluid flow pathways through the shallower sediments [5, 39, 40]. In most cases, these minor faults in the study area are highlighted by obvious broken reflections. Sometimes, fluid flows charged in the minor faults will reduce acoustic velocity and result in apparent downward deflection of otherwise horizontal reflectors, called pull-downs. Both minor faults and pull-downs in the study area occur within the shal-

low strata, and their vertical extents are no more than 150 ms TWT (Figure 6). They occur in different environments, such as those related to the polarity reverse zones (Figure 5(a)) or within the paleochannel (Figure 6(a)). Most of them do not extend to the seafloor, but some minor faults, such as the pull-down above the PR\_B (Figure 6(c)), may pierce the seafloor and provide the pathway for fluid flows into the ocean.

Gas chimneys in the study area are characterized by columnar disrupted zones in the seismic sections (Figures 7–9). Gas hydrates filled in gas chimneys will increase acoustic velocity and result in unusual seismic anomaly features. The reflection events of their flanks are nearly unfaulted at the edge, and their internal events show a regular convex upward geometry. They are different from other ordinary

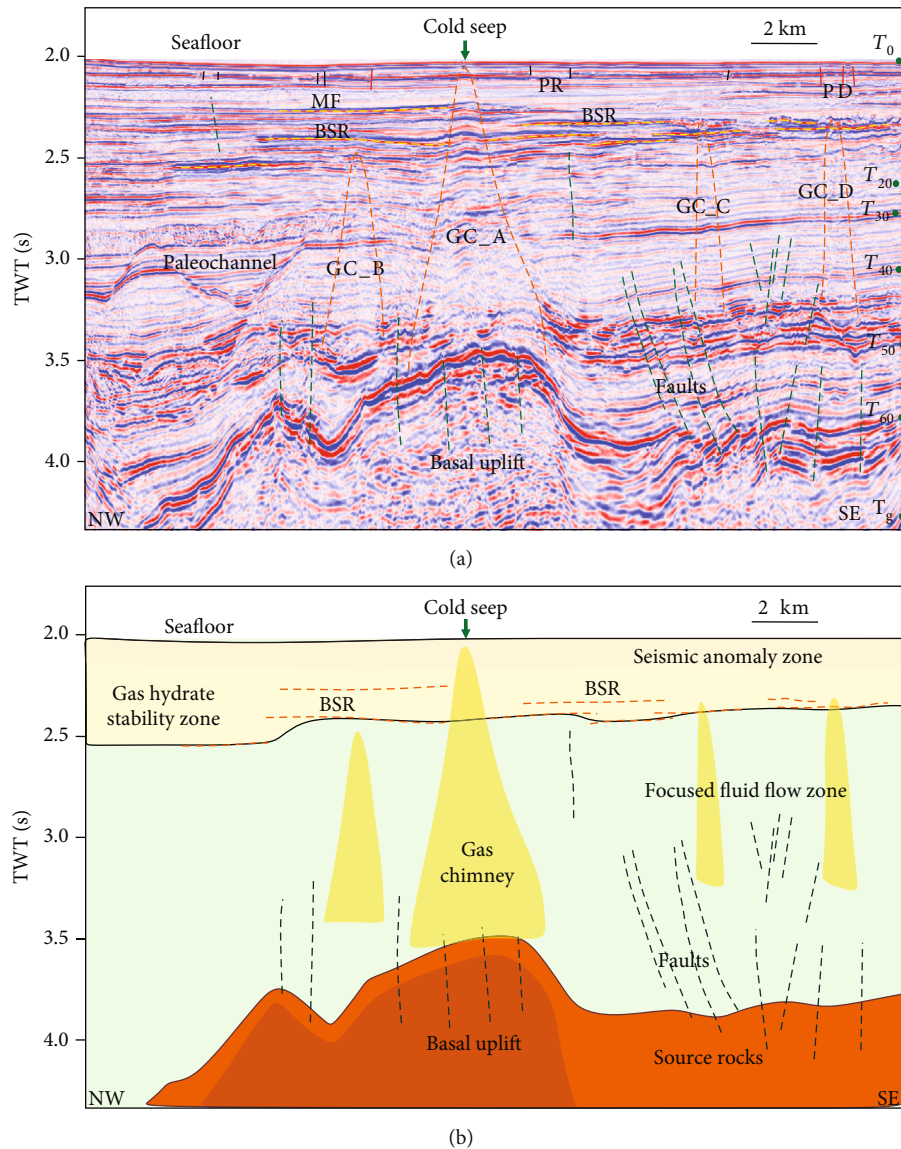


FIGURE 8: (a) Seismic section of the deep gas chimneys, BSRs, and newly discovered cold seeps in the study area and (b) schematic diagram of the gas generation, migration, and accumulation in the study area. The yellow dashed lines in panel (a) indicate the BSRs, the orange dashed lines delineate the gas chimneys, and the olive green lines indicate the faults. The orange area in panel (b) represents Eocene-Oligocene source rocks, and the yellow cones represent gas chimneys; the light green area represents the gas migration zone. The BGHSZ is indicated by BSRs, and the top area is the seismic anomaly area, which is also characterized by focused fluid flows and shallow gas hydrates. PR: polarity reverse; PD: pulldown; MF: minor fault; GC: gas chimney.

gas chimneys, which commonly show chaotic and/or blank reflection patterns caused by gas-charged fluid flows [5]. Shallow gas chimneys mainly develop in the shallow Quaternary strata and are commonly hundreds of meters in diameter, and most of them are observed at 2080~2250 ms TWT, between BSRs and seafloors. Several shallow gas chimneys may develop side by side and form a cluster (Figure 7(e)). Except for these shallow gas chimneys, some chimneys will extend down into deep sediment layers. As shown in Figures 7(d) and 8, the gas chimney\_A (GC\_A) extends straightly down to the basement, while the gas chimney\_B, gas chimney\_C, and gas chimney\_D (GC\_B, GC\_C, and GC\_D) are connected with the basement by faults instead of

directly reaching it. Most of the deep gas chimneys upwardly terminate below the BSRs, and only the GC\_A pierces the seafloor and generates a cold seep in the study area.

**4.2. Newly Discovered Cold Seep.** On the lower continental slope of the northwestern SCS, approximately 50 km north-east of the “Haima” cold seeps, a newly discovered cold seep is situated at ~1520 m water depths (Figures 1(a) and 9(c)), which is connected with the GC\_A. The GC\_A shows columnar vertical convex aligned reflectors in the seismic sections (Figures 7(e), 8, and 9(b)), originates from a basal uplift with an approximate width of 3.5 km, narrows up gradually to less than 1 km, and finally forms a 40 m diameter crater on the

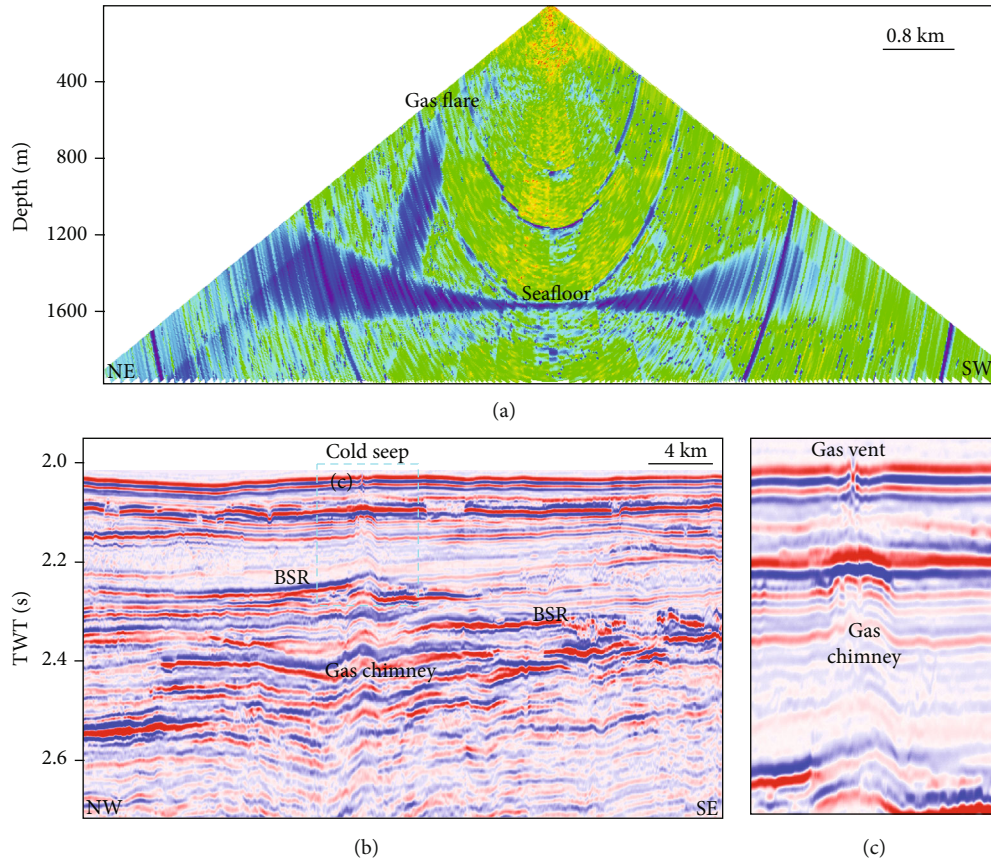


FIGURE 9: (a) Echogram of the gas flare, (b) seismic section, and (c) corresponding amplified map of the newly discovered cold seep in the study area.

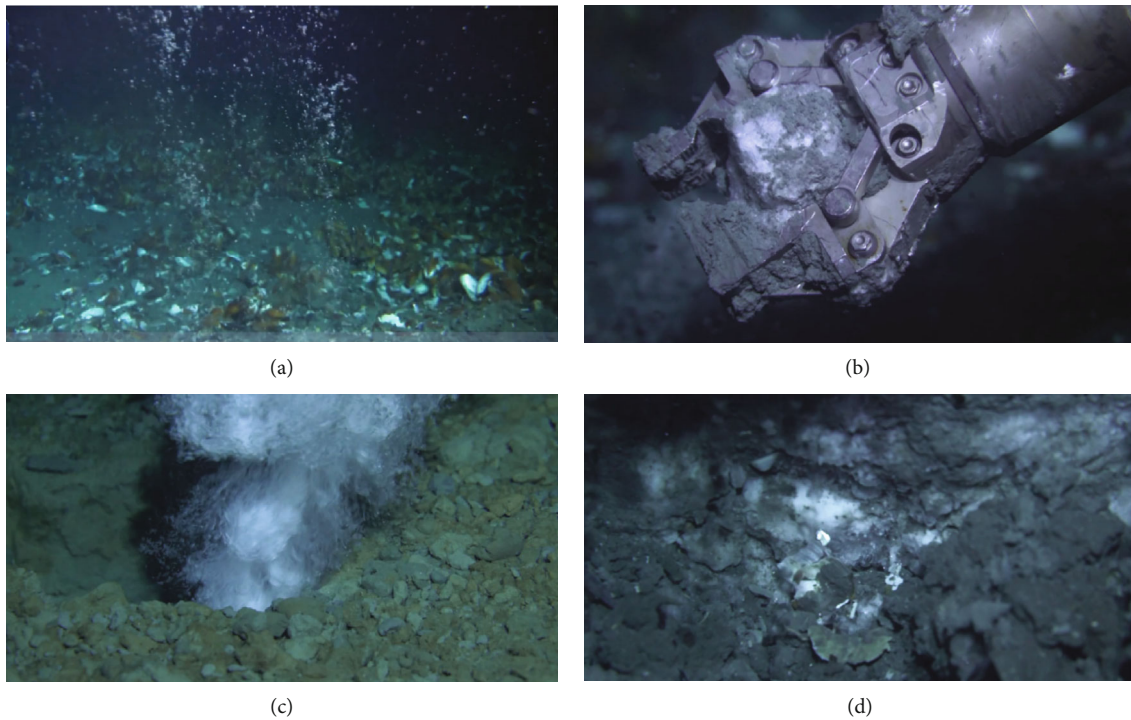


FIGURE 10: Seafloor observations of gas seepages (a, c) and near-surface gas hydrates (b, d) made by ROV "Haima" at the newly discovered active cold seep.

seabed. In addition, a flare-shaped backscatter feature rising about 800 m away from the seafloor, with a width of 400 m, is delineated at this site on the echogram (Figure 9(a)). Observations made with the ROV “Haima” confirm the existence of gas seepages, shallow gas hydrates, and cold seep ecosystems at this site (Figure 10). All these prove the ongoing gas seepage activities at this newly discovered cold seep.

## 5. Discussion

The analysis from the “Haima” cold seeps and the sites GMGS5-W08 and GMGS5-W09, which are located northeast of the study area and drilled during the fifth “China National Gas Hydrate Drilling Expedition” (GMGS5), demonstrates that the hydrate-methanes in the QDNB are mixed gases, and the thermogenic hydrocarbons generated by Eocene and Oligocene Yacheng formations serve as the main sources [8, 13, 34, 41–43]. The geochemical analysis conducted elsewhere in the QDNB also confirms the presence of Eocene and Oligocene source rocks [44]. Certainly, biogenic gases are also involved in this process, as the research studies of Liang et al., Lai et al., and Zhang et al. [8, 34, 45] verify that the self-generation and self-accumulation biogenic gas supply systems develop in the basin. As shown in Figure 8, we propose that the thermogenic gases originated from deep E-O strata migrate upward along deep faults and/or deep gas chimneys, such as GC\_B~D, into the gas hydrate stability zone, which form diffusive gas hydrates indicated by BSRs or a mix of leakage gas hydrate and free gas filled in the minor faults, polarity reverse zones, and gas chimneys. In addition, the thermogenic gases may migrate along the deep gas chimney, such as GC\_A, directly to the seafloor, sustain localized gas seepages, and nourish an active cold seep system. During the hydrocarbon migration, the leakage gas hydrates will be generated under suitable conditions filling in the gas chimneys and result in unusual convex upward reflections within the gas chimney and unfaulted flanks at the edges of the gas chimney. The thermogenic hydrocarbons with the characteristic of lower generation and upper accumulation result in the related seismic anomalies dominantly distributed in the Lingnan Low Uplift (Figure 4). This result provides insight into the relationship between shallow gas hydrate accumulation and deep hydrocarbon generation and migration and simultaneously has important implications for hydrocarbon explorations in the QDNB, northwestern SCS.

## 6. Conclusions

Multiple seismic anomalies, including polarity reverses, pull-downs, minor faults, gas chimneys, and BSRs, are recognized in the central QDNB, northwestern SCS, which indicate intensively distributed shallow gas hydrates, free gas, and focused fluid flows within the shallow strata in the study area. In addition, the newly discovered cold seep related to a deep gas chimney with an internal convex upward geometry also demonstrates ongoing focused fluid flows and shallow gas hydrates at this site. The thermogenic gases originated from deep E-O strata are the main hydrocarbon sources, and they

migrate along deep faults and gas chimneys to the shallower Lingnan Low Uplift and contribute to the genesis of the shallow gas hydrates, cold seeps, and focused fluid flows in the study area. The characteristics and distributions of the seismic evidence indicative of shallow gas hydrates and focused fluid flows provide insights into the understanding of the coupling relationship between seafloor cold seeps, shallow gas hydrates, and focused fluid flows in depth and have important implications for hydrocarbon explorations in the QDNB, northwestern SCS.

## Data Availability

The seismic and other data used to support the findings of this study have not been made available because the data are confidential.

## Conflicts of Interest

The authors declare that they have no conflicts of interest.

## Acknowledgments

We thank the Guangzhou Marine Geological Survey for the permission to release these data for scientific research. This work is supported by the Key Research and Development Project of Guangdong (grant number 2020B1111510001); the Key Special Project for Introduced Talents Team of Southern Marine Science and Engineering Guangdong Laboratory (Guangzhou) (grant number GML2019ZD0207); the Guangdong Basic and Applied Basic Research Foundation (grant number 2019B030302004); the National Key R&D Program of China (grant number 2018YFC0310000); the Project of China Geological Survey (grant number DD20191031); and the State Key Laboratory of Marine Geology, Tongji University (grant number MGK1920). Dr. Shengxiong Yang is funded by the Project of Southern Marine Science and Engineering Guangdong Laboratory (Guangzhou) (project number GML2020GD0802).

## References

- [1] J. Liang, H. Wang, X. Su et al., “Natural gas hydrate formation conditions and the associated controlling factors in the northern slope of the South China Sea,” *Natural Gas Industry*, vol. 34, no. 7, pp. 128–135, 2014.
- [2] R. W. Zhang, H. Q. Li, B. J. Zhang, H. D. Huang, and P. F. Wen, “Detection of gas hydrate sediments using prestack seismic AVA inversion,” *Applied Geophysics*, vol. 12, no. 3, pp. 453–464, 2015.
- [3] J. Wei, Y. Fang, H. Lu et al., “Distribution and characteristics of natural gas hydrates in the Shenhu Sea Area, South China Sea,” *Marine and Petroleum Geology*, vol. 98, pp. 622–628, 2018.
- [4] C. Petersen, S. Bünz, S. Hustoft, J. Mienert, and D. Klaeschen, “High-resolution P-Cable 3D seismic imaging of gas chimney structures in gas hydrated sediments of an Arctic sediment drift,” *Marine and Petroleum Geology*, vol. 27, no. 9, pp. 1981–1994, 2010.
- [5] Q. Sun, S. Wu, J. Cartwright, and D. Dong, “Shallow gas and focused fluid flow systems in the Pearl River Mouth Basin,

- northern South China Sea,” *Marine Geology*, vol. 315-318, pp. 1–14, 2012.
- [6] G. Panieri, S. Bünz, D. Fornari et al., “An integrated view of the methane system in the pockmarks at Vestnesa Ridge, 79°N,” *Marine Geology*, vol. 390, pp. 282–300, 2017.
- [7] J. Greinert, J. Bialas, K. Lewis, and E. Suess, “Methane seeps at the Hikurangi Margin, New Zealand,” *Marine Geology*, vol. 272, no. 1-4, pp. 1–3, 2010.
- [8] J. Liang, W. Zhang, J. Lu, J. Wei, Z. Kuang, and Y. He, “Geological occurrence and accumulation mechanism of natural gas hydrates in the eastern Qiongdongnan Basin of the South China Sea: insights from site GMGS5-W9-2018,” *Marine Geology*, vol. 418, article 106042, 2019.
- [9] J. He, Y. Zhu, S. Chen, Y. Zhu, S. Cui, and W. Ma, “Genetic types and mineralization characteristics of gas hydrate and resources potential of northern South China Sea,” *Natural Gas Geoscience*, vol. 20, no. 2, pp. 237–243, 2009.
- [10] P. Yan and D. Chen, “New geophysical evidence for gas hydrates in Baiyun Sag in the northern margin of the South China Sea,” *Journal of Tropical Oceanography*, vol. 28, no. 3, pp. 85–85, 2009.
- [11] N. Wu, G. Zhang, J. Liang et al., “Progress of gas hydrate research in northern South China Sea,” *Advances in New and Renewable Energy*, vol. 1, no. 1, pp. 80–94, 2013.
- [12] D. Chen, Z. Su, D. Feng, and L. Cathles, “Formation and its controlling factors of gas hydrate reservoir in marine gas vent system,” *Journal of Tropical Oceanography*, vol. 24, no. 3, pp. 38–46, 2005.
- [13] D. Wei, L. Jinqiang, Z. Wei, K. Zenggui, Z. Tong, and H. Yulin, “Typical characteristics of fracture-filling hydrate-charged reservoirs caused by heterogeneous fluid flow in the Qiongdongnan Basin, northern South China Sea,” *Marine and Petroleum Geology*, vol. 124, article 104810, 2021.
- [14] Q. Liang, Y. Hu, D. Feng et al., “Authigenic carbonates from newly discovered active cold seeps on the northwestern slope of the South China Sea: constraints on fluid sources, formation environments, and seepage dynamics,” *Deep Sea Research Part I: Oceanographic Research Papers*, vol. 124, pp. 31–41, 2017.
- [15] C. Liu, S. Morita, Y. Liao et al., “High resolution seismic images of the Formosa Ridge off southwestern Taiwan where “hydrothermal” chemosynthetic community is present at a cold seep site,” in *Proceedings of the 6th international conference on gas hydrates (ICGH 2008)*, Vancouver, British Columbia, Canada, 2008.
- [16] D. Feng and D. Chen, “Authigenic carbonates from an active cold seep of the northern South China Sea: new insights into fluid sources and past seepage activity,” *Deep Sea Research Part II: Topical Studies in Oceanography*, vol. 122, pp. 74–83, 2015.
- [17] K. Ru and J. Pigott, “Episodic rifting and subsidence in the South China Sea,” *AAPG Bulletin*, vol. 70, pp. 1136–1155, 1986.
- [18] Z. Gong and S. Li, “Continental margin basin analysis and hydrocarbon accumulation of the northern South China Sea,” Science Press, 1997.
- [19] M. Zhao, X. Zhang, L. Ji, and G. Zhang, “Characteristics of tectonic evolution in the Qiongdongnan Basin and brief discussion about its controlling on reservoirs,” *Natural Gas Geoscience*, vol. 21, no. 3, pp. 494–502, 2010.
- [20] B. Huang, H. Tian, X. Li, Z. Wang, and X. Xiao, “Geochemistry, origin and accumulation of natural gases in the deepwater area of the Qiongdongnan Basin, South China Sea,” *Marine and Petroleum Geology*, vol. 72, pp. 254–267, 2016.
- [21] A. Su, H. Chen, X. Chen, H. Liu, Y. Liu, and M. Lei, “New insight into origin, accumulation and escape of natural gas in the Songdong and Baodao regions in the eastern Qiongdongnan Basin, South China Sea,” *Journal of Natural Gas Science and Engineering*, vol. 52, pp. 467–483, 2018.
- [22] Z. Zhao, Z. Sun, Z. Wang, Z. Sun, J. Liu, and C. Zhang, “The high resolution sedimentary filling in Qiongdongnan Basin, northern South China Sea,” *Marine Geology*, vol. 361, pp. 11–24, 2015.
- [23] Z. Zhao, Z. Sun, L. Sun, Z. Wang, and Z. Sun, “Cenozoic tectonic subsidence in the Qiongdongnan Basin, northern South China Sea,” *Basin Research*, vol. 30, no. S1, pp. 269–288, 2016.
- [24] X. Wang, S. Wu, D. Dong, Y. Guo, and H. Deborah, “Control of mass transport deposits over the occurrence of gas hydrate in Qiongdongnan Basin,” *Marine Geology and Quaternary Geology*, vol. 31, no. 1, pp. 109–118, 2011.
- [25] J. Wang, S. Wu, X. Kong et al., “Subsurface fluid flow at an active cold seep area in the Qiongdongnan Basin, northern South China Sea,” *Journal of Asian Earth Sciences*, vol. 168, pp. 17–26, 2018.
- [26] X. Xie, Z. Wang, S. Li, M. Zhang, and J. Yang, “Characteristics of overpressure systems and their significance in hydrocarbon accumulation in the Yinggehai and Qiongdongnan Basins, China,” *Acta Geologica Sinica*, vol. 77, no. 2, pp. 258–266, 2003.
- [27] J. He, S. Chen, H. Liu, and S. Liu, “Petroleum resource potential and advantageous exploration targets in Ying-Qiong Basin, northern margin of South China Sea,” *Natural Gas Geoscience*, vol. 19, no. 4, pp. 492–498, 2008.
- [28] X. Wang, S. Wu, S. Yuan et al., “Geophysical signatures associated with fluid flow and gas hydrate occurrence in a tectonically quiescent sequence, Qiongdongnan Basin, South China Sea,” *Geofluids*, vol. 10, no. 3, 368 pages, 2010.
- [29] P. Zhai and H. Chen, “Discharging zones of overpressure system in Qiongdongnan Basin, northern South China Sea: implications for favorable sites of natural gas accumulation,” *Earth Science-Journal of China University of Geosciences*, vol. 38, no. 4, pp. 832–842, 2013.
- [30] W. Zhu, “Petroleum geology in deepwater area of northern continental margin in South China Sea,” *Acta Petrolei Sinica*, vol. 31, no. 4, pp. 521–527, 2010.
- [31] X. Shi, H. Jiang, J. Yang, X. Yang, and H. Xu, “Models of the rapid post-rift subsidence in the eastern Qiongdongnan Basin, South China Sea: implications for the development of the deep thermal anomaly,” *Basin Research*, vol. 29, no. 3, pp. 340–362, 2017.
- [32] G. Zhang, Y. Zhang, H. Shen, and Y. He, “An analysis of natural gas exploration potential in the Qiongdongnan Basin by use of the theory of joint control of source rock and geothermal heat,” *Natural Gas Industry*, vol. 34, no. 1, pp. 18–27, 2014.
- [33] P. D. Clift and Z. Sun, “The sedimentary and tectonic evolution of the Yinggehai–Song Hong Basin and the southern Hainan margin, South China Sea: implications for Tibetan uplift and monsoon intensification,” *Journal of Geophysical Research*, vol. 111, article B06405, 2006.
- [34] H. Lai, Y. Fang, Z. Kuang et al., “Geochemistry, origin and accumulation of natural gas hydrates in the Qiongdongnan Basin, South China Sea: implications from site GMGS5-

- W08,” *Marine and Petroleum Geology*, vol. 123, article 104774, 2021.
- [35] O. Yilmaz and S. M. Doherty, *Seismic Data Analysis: Processing, Inversion, and Interpretation of Seismic Data*, Society of exploration geophysicists- Investigations in Geophysics, Tulsa, Okla, 2001.
- [36] S. Garcia-Gil, F. Vilas, and A. Garcia-Garcia, “Shallow gas features in incised-valley fills (Ría de Vigo, NW Spain): a case study,” *Continental Shelf Research*, vol. 22, no. 16, pp. 2303–2315, 2002.
- [37] R. J. Evans, S. A. Stewart, and R. J. Davies, “Phase-reversed seabed reflections in seismic data: examples related to mud volcanoes from the South Caspian Sea,” *Geo-Marine Letter*, vol. 27, no. 2-4, pp. 203–212, 2007.
- [38] Z. Tóth, V. Spieß, and J. Jensen, “Seismo-acoustic signatures of shallow free gas in the Bornholm Basin, Baltic Sea,” *Continental Shelf Research*, vol. 88, pp. 228–239, 2014.
- [39] S. Haines, P. Hart, T. Collett et al., “High-resolution seismic characterization of the gas and gas hydrate system at Green Canyon 955, Gulf of Mexico, USA,” *Marine and Petroleum Geology*, vol. 82, pp. 220–237, 2017.
- [40] J. Wei, J. Liang, J. Lu, W. Zhang, and Y. He, “Characteristics and dynamics of gas hydrate systems in the northwestern South China Sea - results of the fifth gas hydrate drilling expedition,” *Marine and Petroleum Geology*, vol. 110, pp. 287–298, 2019.
- [41] Q. Sun, J. Cartwright, M. Foschi, X. Lu, and X. Xie, “The interplay of stratal and vertical migration pathways in shallow hydrocarbon plumbing systems,” *Basin Research*, vol. 33, pp. 1–22, 2021.
- [42] J. Wei, T. Wu, L. Zhu et al., “Mixed gas sources induced co-existence of sI and sII gas hydrates in the Qiongdongnan Basin, South China Sea,” *Marine and Petroleum Geology*, vol. 128, p. 105024, 2021.
- [43] W. Zhang, J. Liang, J. Lu et al., “Characteristics and controlling mechanism of typical leakage gas hydrate reservoir forming system in the Qiongdongnan Basin, northern South China Sea,” *Natural Gas Industry*, vol. 40, no. 8, pp. 90–99, 2020.
- [44] L. Wang, J. Zhu, H. Zhuo et al., “Seismic characteristics and mechanism of fluid flow structures in the central depression of Qiongdongnan Basin, northern margin of South China Sea,” *International Geology Review*, vol. 62, pp. 1108–1130, 2020.
- [45] W. Zhang, J. Liang, P. Su et al., “Distribution and characteristics of mud diapirs, gas chimneys, and bottom simulating reflectors associated with hydrocarbon migration and gas hydrate accumulation in the Qiongdongnan Basin, northern slope of the South China Sea,” *Geological Journal*, vol. 54, no. 6, pp. 3556–3573, 2019.